

**A Q-SWITCHED, CAVITY-DUMPED YAG LASER
FOR USE IN PLASMA PHYSICS EXPERIMENTS**

by

STEVEN ROY LEFFLER

B.Sc. (Honours Physics), The University of Western Ontario, 1990

A THESIS SUBMITTED IN PARTIAL FULFILLMENT OF

THE REQUIREMENTS FOR THE DEGREE OF

MASTER OF SCIENCE

in

THE FACULTY OF GRADUATE STUDIES

DEPARTMENT OF PHYSICS

We accept this thesis as conforming

to the required standard



THE UNIVERSITY OF BRITISH COLUMBIA

December 1992

© Steven Roy Leffler, 1992

In presenting this thesis in partial fulfilment of the requirements for an advanced degree at the University of British Columbia, I agree that the Library shall make it freely available for reference and study. I further agree that permission for extensive copying of this thesis for scholarly purposes may be granted by the head of my department or by his or her representatives. It is understood that copying or publication of this thesis for financial gain shall not be allowed without my written permission.

(Signature)



Department of Physics

The University of British Columbia
Vancouver, Canada

Date December 18, 1992

Abstract

A Q-switched, cavity-dumped Nd:YAG laser was developed for use as a diagnostic tool in plasma physics experiments. This laser uses an unstable resonator configuration to produce higher gain and better collimation than would otherwise be possible. Pulses of light with energies of 18 ± 2 mJ and FWHMs of about 12 ns were produced.

It was found that more than 100 mJ of light was being emitted in the form of pre-lase pulses, due to the Pockels cells used having a poor extinction ratio. Efforts were made to correct this problem, with only partial success.

Table of Contents

Abstract	ii
List of Figures	v
Acknowledgements	vii
1. Introduction	1
1.1 Motivation	1
1.2 Summary of Project	2
1.3 Outline of the Thesis	3
2. Theory	5
2.1 Introduction	5
2.2 The Lasing Medium	5
2.3 Unstable Resonators	7
2.3.1 Introduction to Unstable Resonators	7
2.3.2 Loss Calculation for Unstable Resonators	11
2.4 Q-Switching	14
2.4.1 Introduction to Q-Switching	14
2.4.2 Q-Switched Pulse Characteristics	15
2.5 Cavity Dumping	17

3. System Development	20
3.1 Introduction	20
3.2 Initial Design	20
3.2.1 Optical Components	20
3.2.2 Flashtube Pumping	23
3.2.3 Timing and Triggering	25
3.2.4 Expected Performance	28
3.3 Tests and Design Modifications	30
3.3.1 Preliminary Tests	30
3.3.2 Optimization of Output	33
3.3.3 Attempts to Diagnose and Correct the Pockels Cell Problem	36
4. Conclusions	47
List of References	49

List of Figures

Figure 2.1: Simplified energy level diagram for Nd:YAG	6
Figure 2.2: Some examples of stable and unstable resonators. (a) Two commonly-used stable resonator configurations. (b) Two unstable resonator configurations.	9
Figure 2.3: Graph of unstable resonator loss due to "diffraction", as a function of the product of the mirrors' curvature parameters.	12
Figure 3.1: Schematic diagram of the initial YAG laser cavity layout.	21
Figure 3.2: Schematic of the initial Pockels cell triggering circuit design.	27
Figure 3.3: Variation of cavity-dumped output energy with Pockels cell voltage. Each point is an average of 5 shots. The curve is a weighted least-squares fit to the data, excluding the four anomalously low points.	34
Figure 3.4: Schematic of Pockels cell control circuit with simplified cavity dump system.	38
Figure 3.5: Schematic diagram of final YAG laser cavity layout, with Pockels cell control circuit.	40
Figure 3.6: Light in the laser cavity (lower trace) and its integral (upper trace). Horizontal scale is 10 μ s/division. Vertical scales are arbitrary.	42

Figure 3.7: Observed and expected reflection of HeNe light by an apparatus consisting of a Pockels cell placed between a plane mirror and a polarizer. The theoretical curve is normalized to the same peak intensity as the observed data. 45

Acknowledgements

I would like to thank my supervisor, Jochen Meyer, for his constant encouragement and support. I've learned a lot under his guidance. I would also like to thank Abdul Elezzabi, Michael Hughes, Ross McKenna, and Peter Zhu for many interesting and useful conversations about lasers, physics, and life in general. Al Cheuck helped with the electronics. Dr. Andrew Ng provided the saturable absorbing dye which I experimented with in an attempt to improve the laser's performance. Andrew Forsman gave a lot of advice on how best to prepare and use the dye.

I would especially like to thank Hubert Houtman, who laid much of the groundwork for this project prior to my joining the lab, including fabricating the laser head and some of the other components. Hubert also provided a great deal of useful advice on the practical side of building a laser and getting it to work.

Thanks are also due to my family for their support and encouragement, and to the gang at the Lutheran Campus Centre for just being there.

The Natural Sciences and Engineering Research Council of Canada supported my first two years of study through their "Postgraduate Scholarships" program.

Chapter 1

Introduction

1.1 Motivation

In most of the plasma physics research done in our lab, experiments are carried out on plasmas generated by ablating material with a 12 J pulse of infrared light from a CO₂ laser system. The primary diagnostic tool in these experiments is a ruby laser which produces 6 ns long pulses with energies around 800 mJ. These pulses undergo Thompson scattering off Langmuir waves in the plasma. The scattered light is then analyzed to ascertain the values of the parameters of the plasma which are relevant to the experiment being carried out.

The principal detector used in these experiments is a Hamamatsu streak camera, which has a quantum efficiency which peaks for light whose wavelength is around 420 nm. The range of wavelengths for which this detector's quantum efficiency is better than 5% extends from about 300 nm to about 530 nm. Since ruby lasers produce light with a wavelength of 694.3 nm, the quantum efficiency of the streak camera for ruby laser light is relatively low (around 1.5%). This means that faint scattered signals are often difficult or impossible to detect, and the problem is even worse when the scattering process causes the light to be shifted to a longer wavelength by doppler effects.

It was decided that it was not worthwhile to attempt to obtain a streak camera with a higher sensitivity in the red, because this seemed likely to be expensive, if such a camera were available at all. Instead, the ruby laser would be replaced by a laser which produces light with a wavelength closer to the middle of the current camera's response curve. This thesis describes the construction and testing of a laser to meet this need.

1.2 Summary of Project

The lasing medium chosen for the new laser was neodymium YAG, which produces near infrared light with a wavelength of 1.0641 μm . This light can then be frequency-doubled fairly efficiently to produce green light at 532 nm. At this wavelength, the streak camera's quantum efficiency will be about 5%, so one would expect that for a given amount of input laser power, the response with a frequency-doubled YAG laser would be over three times that obtained with a ruby laser, making it easier to measure faint signals.

In addition to producing a more useful wavelength of light, YAG lasers produce a much higher gain for a given amount of input energy. This means that for the laser to produce the same intensity of light as the old ruby system, it needs a much smaller bank of capacitors to produce the pulse of energy which generates the initial inversion. This simplifies the design of the laser and reduces its cooling requirements considerably.

The initial design goals for the laser were that it was to produce a pulse of light of approximately 6 ns duration, with a total energy in the infrared of 50-100 mJ. This would be sufficient to allow amplification to around 1 J via an amplifier to be added later. It was also desired that the beam be quite well collimated, because it would have to travel several metres in order to reach the experimental target chamber and enter it from an appropriate direction. An additional requirement was that it had to be possible to accurately synchronize the firing of the laser with a control pulse, so that the laser could be set up to fire at a fixed time relative to the firing of the CO₂ laser which generates the plasma being studied.

In order to produce pulses of the duration required, it is necessary to both Q-switch and cavity dump the laser. These techniques both involve varying the optical losses in the

cavity with time, so as to cause the laser to produce a brief pulse of light rather than a continuous beam. The theory behind this is described in Chapter 2.

Because of the collimation requirement, and because high-quality mirrors of appropriate curvature were already on hand in the lab, an unstable resonator configuration was chosen. As will be discussed in section 2.3, unstable resonators produce very well-collimated beams, as well as having other practical advantages over stable resonators in some circumstances.

In order to allow for synchronization with the existing experimental setup, it was decided that an ultraviolet-triggered spark gap should be used to control the timing of the lasing sequence. This allows the laser to be triggered by the same voltage pulse that triggers the spark gaps in the CO₂ laser and its amplifiers, with the relative timing controlled by the length of delay cable between the last CO₂ spark gap and the YAG spark gap.

The laser was not frequency-doubled as part of the work described here, but the crystal for doing so has been obtained and will be added, external to the laser itself, at a later date. The technology of frequency doubling will not be discussed further in this thesis.

1.3 Outline of the Thesis

The remainder of this thesis is organized as follows:

In Chapter 2 is found an explanation of some of the laser physics techniques used in the laser described here, along with formulas for various important parameters that describe the expected performance of the laser. The chapter begins with a brief description of the lasing medium used, Nd³⁺:YAG. It goes on to describe some of the features of unstable resonators, and to explain why they are useful. Formulas describing the loss of light in this

type of resonator are given, for use later in the thesis. Next, the technique of Q-switching is described, along with formulas for the energy and duration of pulses produced using this technique. Finally, the chapter explains the technique of cavity dumping, which is used to produce shorter pulses than would otherwise be possible.

Chapter 3 explains the initial design for the laser, and makes some estimates of the performance to be expected from it. The chapter then goes on to describe the tests that were run on the laser and the modifications to the initial design that were made due to the results of these tests. A problem with the Pockels cells used for Q-switching and cavity dumping was found, and the chapter concludes with a description of the various attempts that were made to diagnose and correct this problem. In the end, the cause of the problem was found, but it was not completely solved.

In Chapter 4, the results obtained are summarized and suggestions for further work to improve the laser are presented, including suggestions of ways to correct the Pockels cell performance problems.

Chapter 2

Theory

2.1 Introduction

This chapter contains a summary of those aspects of laser physics which are relevant to the operation of a Q-switched, cavity-dumped Nd:YAG laser with an unstable resonator. It is assumed that the reader is already familiar with the basic structure and principles of operation of a simple continuous-wave (CW) laser.

The effects of using an unstable resonator, of Q-switching, and of cavity dumping can for the most part be treated independently, so in this chapter there are separate sections on each of these techniques, as well as one on the Nd:YAG lasing medium itself.

2.2 The Lasing Medium

The lasing medium commonly referred to as "neodymium YAG" or "YAG" is crystalline, and is composed of yttrium aluminum garnet ($Y_3Al_5O_{12}$), with trivalent neodymium replacing up to 1.5% of the yttrium atoms in the crystal's structure. This is usually written Nd^{3+} :YAG, or simply Nd:YAG. It was first successfully made to lase by Geusic, Marcos, and Van Uitert [1].

Nd:YAG is a very useful lasing material because of its good physical and chemical properties, most notably that it is strong and hard enough to be cut and polished without severe breakage problems, and that its high thermal conductivity ($0.13 \text{ W cm}^{-1} \text{ K}^{-1}$ at 300 K) allows for efficient cooling during operation. Also, for a given amount of input energy, Nd:YAG produces a much higher gain than many other solid-state lasing materials. Its index

of refraction for wavelengths around 1 μm is 1.82. Koechner [2] summarizes many other physical and optical properties of Nd:YAG which are not relevant to the operation of the laser described in this thesis, and compares Nd:YAG with other common solid-state lasing media.

At room temperature, the dominant line in the Nd:YAG fluorescence spectrum is at 1.0641 μm , and therefore only this frequency will lase under most conditions. Nd:YAG can, however, be made to lase on other lines in its spectrum if a dispersive prism or other frequency-selecting device is placed within the laser cavity. The alternative lines with the lowest thresholds for lasing are at 1.0615 μm and 1.0738 μm .

All three of the lines mentioned arise from transitions between various components of the $^4F_{3/2}$ and $^4I_{11/2}$ manifolds. A simplified energy-level diagram for Nd:YAG is shown in Figure 2.1, with the dominant laser transition marked.

The process by which YAG lases at 1.0641 μm is as follows: a powerful lamp is used to provide energy to the YAG rod. Visible-light photons from the lamp are absorbed in the rod, exciting electrons from the ground state to the "pump bands", which lie between 18 000 and 25 000 cm^{-1} (2.2 - 3.1 eV). These electrons rapidly decay to the $^4F_{3/2}$ energy level, which has a radiative lifetime of 550 μs . This is called the upper laser level. The laser transition is to the $^4I_{11/2}$ level (the "lower laser level"), which has a lifetime for decay to the ground state of 30 ns.

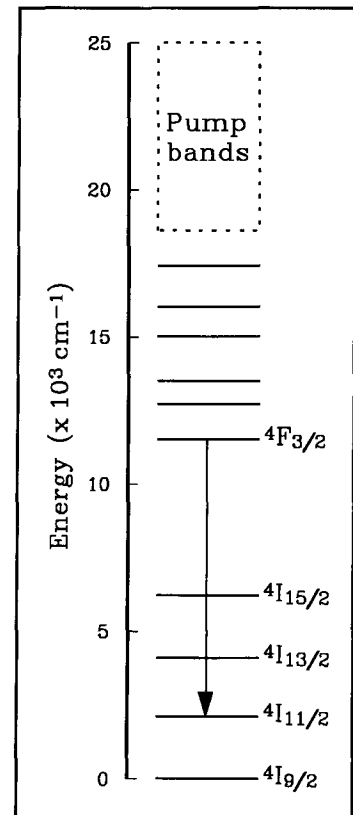


Figure 2.1: Simplified energy level diagram for Nd:YAG

In addition to having a fast decay to the ground state, the lower laser level in Nd:YAG has a high enough energy to be essentially unpopulated in thermal equilibrium at room temperature. These qualities make YAG a "four-level" lasing medium, so called because there are four distinct energy levels involved in the lasing process. This is very important because it prevents electrons from accumulating in the lower laser level during operation, which would reduce the gain of the laser considerably because of the ability of these electrons to absorb photons at the laser frequency (which excites the electrons back up to the upper laser level).

2.3 Unstable Resonators

2.3.1 Introduction to Unstable Resonators

An essential element of all lasers is the *resonator*: a set of mirrors which confine the light in the laser so that it can be repetitively amplified by the lasing medium. In most lasers, the resonator is composed of two mirrors, which are either planar or spherical. Generally, the cavity length (or mirror separation) and mirror curvatures are chosen such that the resonator is stable. This means that there exist modes where the light is completely confined by the mirrors, in the sense that a ray propagating according to geometric optics would bounce back and forth between the mirrors indefinitely and never escape past their edges, as illustrated in Figure 2.2 (a). In these resonators, the only mirror-related losses are those due to transmission through the mirrors and diffraction of light past their edges, both of which can be minimized by choosing mirrors of suitable size and quality. A resonator is stable if it satisfies the relation

$$0 \leq g_1 g_2 \leq 1 \quad (2.1)$$

where $g_i \equiv 1 - L/R_i$ is the curvature parameter for mirror i ,

L is the mirror separation,

and R_i is the radius of curvature of mirror i , defined such that $R_i > 0$ if the centre of curvature of mirror i lies in the direction of the other mirror.

One of the disadvantages of stable resonators is that the diameters of the modes of light which survive in them are almost invariably quite small, because off-axis light tends to be redirected back towards the centre of the beam, except in neutrally stable resonators such as the plane-plane type. Yariv [3] solves Maxwell's equations for the case of a beam of light whose radial intensity distribution is Gaussian, and develops from it a technique for calculating the form of the lowest-order modes in an optical resonator. This analysis confirms that the diameter tends to be relatively small (under a few millimetres). The small mode diameter in stable resonators reduces the gain of the laser, because only a small portion of the volume of the lasing medium can be used for amplification of the light.

One way of increasing the active volume of lasing material is to use an unstable resonator, ie. one where the cavity length and mirror curvatures do not satisfy equation (2.1). In these resonators, any ray of light which is not exactly on the central axis of the resonator will get farther from it on each bounce, until it eventually misses one of the mirrors and leaves the cavity, as shown in Figure 2.2 (b). This leads to much higher losses than in the case of a stable resonator, but a much larger beam diameter. If the increase in gain due to the increased beam diameter is large enough to compensate for the increased diffraction

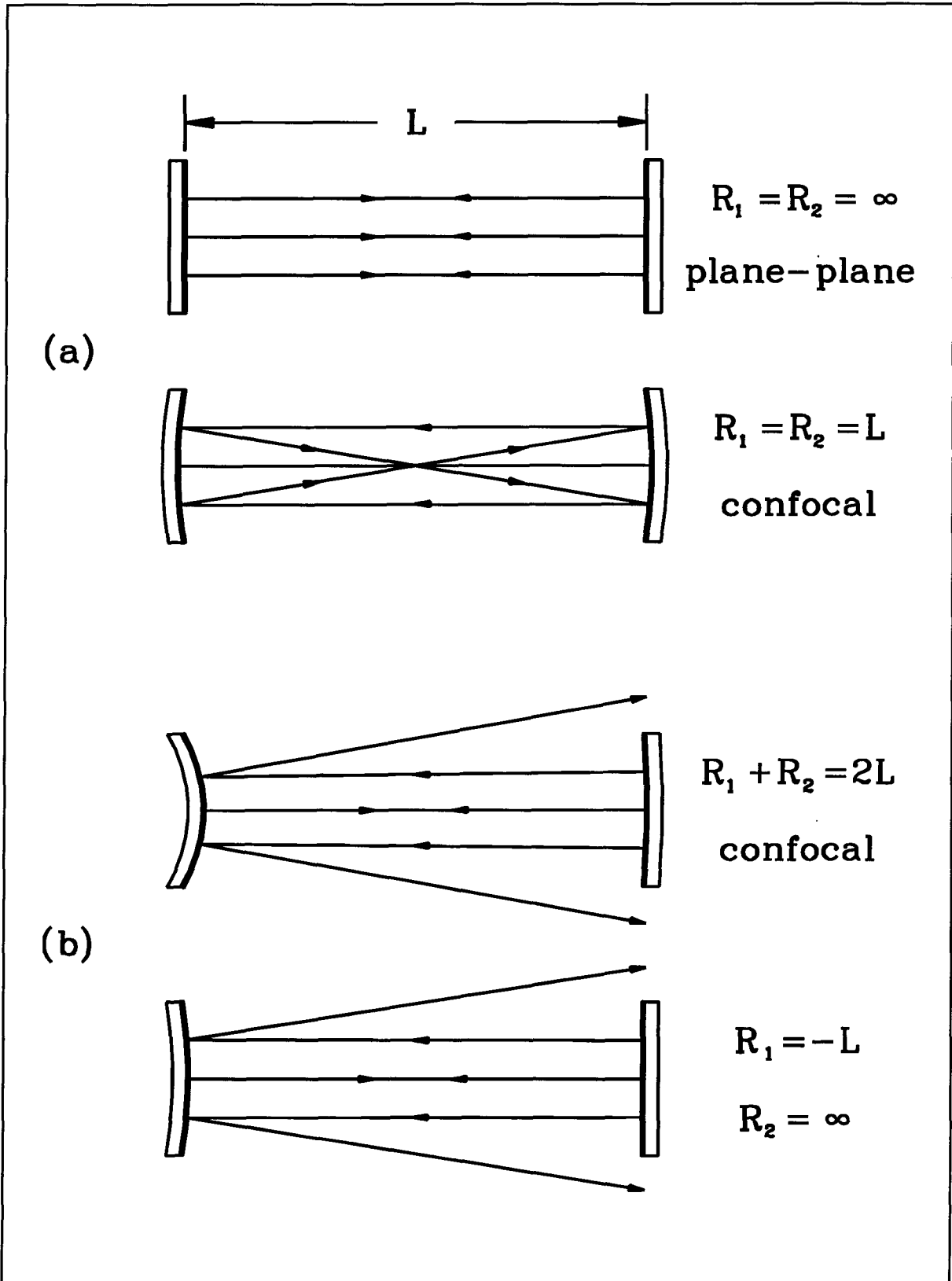


Figure 2.2: Some examples of stable and unstable resonators. (a) Two commonly-used stable resonator configurations. (b) Two unstable resonator configurations.

losses*, using an unstable resonator can be worthwhile.

Unstable resonators also have the advantage of providing some control over the transverse modes. Because light which is propagating off-axis in the resonator is lost more quickly than light which is propagating on-axis, these resonators favour the TEM_{00} mode over other TEM modes, because it has more of its energy concentrated at the centre of the beam. The TEM_{00} mode is preferable for many applications because it produces a single-phase, radially-symmetric output beam whose intensity as a function of radial distance is Gaussian. This is in contrast to the higher-order modes, which have a much more complicated structure.

A third advantage is that if the mirror curvatures are chosen such that the resonator is confocal, the output beam will be extremely well collimated [4]. The improved collimation occurs because the modes in an unstable resonator are wider than those in a stable resonator, and the limit on beam divergence in the far field imposed by diffraction† scales according to:

$$\theta \propto \frac{\lambda}{D} \quad (2.2)$$

where θ is the far-field apex angle of the beam cone,

λ is the wavelength of the radiation,

and D characterizes the diameter of the output beam.

Large-diameter beams can thus have a lower divergence in the far-field.

* It is conventional to refer to the loss of light past the edges of the mirrors in an unstable resonator as "diffraction loss", even though it arises primarily from geometric optics considerations.

† Diffraction in the ordinary sense of the word.

2.3.2 Loss Calculation for Unstable Resonators

Siegman [5] used geometric optics to produce an approximate expression for the energy loss due to "diffraction" in an unstable resonator. His approach was to assume that the light coming from each mirror has the form of a spherical wave of uniform intensity, with a virtual centre which is not necessarily the centre of curvature of the mirror the light is coming from. By requiring that each virtual centre be the image of the other, on reflection from the appropriate mirror, he was able to derive expressions for the locations of the virtual centres given the radii of curvature of the mirrors and their separation. From these, he was able to estimate the amount of energy lost per "bounce" by examining how much of each spherical wave was intercepted by the opposing mirror. This gives the result that the average single-pass fractional intensity loss, \mathcal{L}_{diff} , is given by

$$\mathcal{L}_{diff} \approx 1 \mp \frac{1 - \sqrt{1 - (g_1 g_2)^{-1}}}{1 + \sqrt{1 - (g_1 g_2)^{-1}}} \quad (2.3)$$

where the upper sign is to be taken when $g_1 g_2 > 1$, and the lower sign is to be taken when $g_1 g_2 < 0$. The equation is, of course, not valid for other values of $g_1 g_2$, since these correspond to stable resonators according to equation (2.1). The former equation is plotted as a function of $g_1 g_2$ in Figure 2.3.

Equation (2.3) is valid for any unstable resonator whose mirrors have spherical curvature, regardless of the size or shape of those mirrors, provided that the Fresnel number of the resonator is large ($N \equiv a^2/L\lambda \gg 1$, where a is the radius of the mirrors). The only other restriction on the form of the mirrors is that they must both extend past the centreline of the resonator.

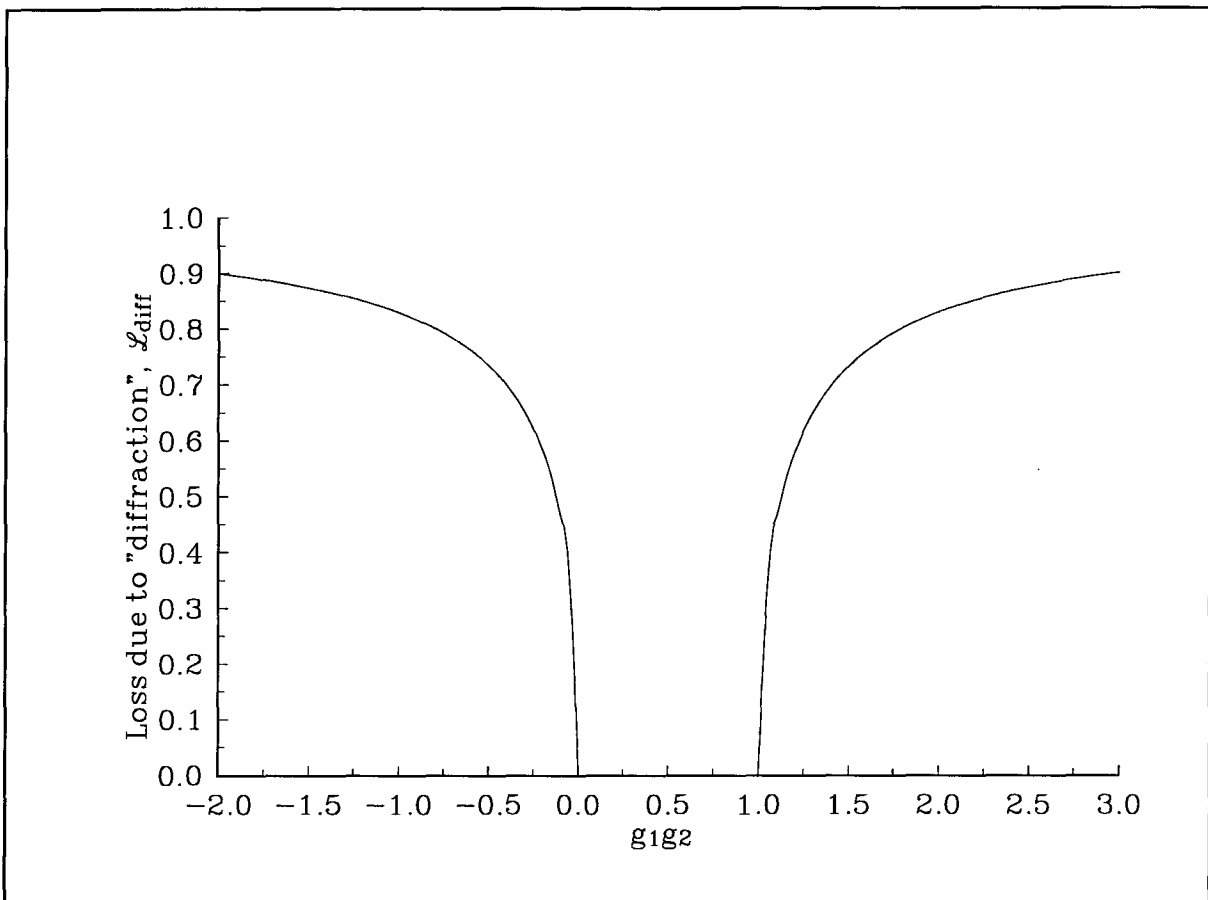


Figure 2.3: Graph of unstable resonator loss due to "diffraction", as a function of the product of the mirrors' curvature parameters.

A more detailed treatment of unstable resonator losses, which includes actual diffraction effects, can be found in Siegman's book [6]. For the purpose of evaluating the performance of the laser described in this thesis, the simpler analysis which results in equation (2.3) is satisfactory, however.

The average loss per pass in a resonator due to sources other than diffraction is given by:

$$\mathcal{L}_{nd} \approx \alpha L - \ln \sqrt{r_1 r_2}, \quad \text{for } \mathcal{L}_{nd} \ll 1 \quad (2.4)$$

where α is the exponential decay constant for distributed losses in the cavity,

and r_i is the intensity reflectivity of mirror i .

This combines with the diffraction loss from equation (2.3) according to the formula

$$\mathcal{L} = \mathcal{L}_{nd} + \mathcal{L}_{diff} - \mathcal{L}_{nd} \mathcal{L}_{diff} \quad (2.5)$$

to give the total loss for the resonator, \mathcal{L} . For most unstable resonators with high-reflectivity mirrors, $\mathcal{L} \approx \mathcal{L}_{diff}$.

A useful parameter for summarizing the losses in a resonator is the *photon lifetime*, t_c . This is the time needed for the energy of the light in the cavity to decrease to 1/e of its initial value, in the absence of any gain mechanism, i.e.

$$\frac{d\mathcal{E}}{dt} = -\frac{\mathcal{E}}{t_c} \quad (2.6)$$

where \mathcal{E} is the energy stored in the cavity.

The relative rate of decrease in energy due to cavity losses is just the fractional loss per pass, \mathfrak{L} , divided by the time needed for light to pass through the cavity once:

$$\frac{1}{\mathcal{E}} \frac{d\mathcal{E}}{dt} = -\frac{c\mathfrak{L}}{nL} \quad (2.7)$$

where nL is the optical path length of the cavity,

and c is the speed of light.

Therefore, the photon lifetime is given by

$$t_c = \frac{nL}{c\mathfrak{L}} \quad (2.8)$$

2.4 Q-Switching

2.4.1 Introduction to Q-Switching

The technique called *Q-switching* is often used to allow the production of short, intense pulses from lasers. It works [7] by temporarily increasing the losses in the cavity while the lasing medium is being pumped, allowing the inversion of the medium to build up to a level much higher than the threshold where lasing would normally start to occur. Once pumping is complete, the losses are lowered to their normal value. Because the inversion is then much higher than the threshold for lasing, light builds up very rapidly in the cavity, resulting in a laser pulse with a very short risetime. After the initial inversion is depleted, the light level in the cavity decays exponentially, with a time constant roughly equal to the photon lifetime, t_c .

Because light builds up rapidly in the cavity during Q-switched operation, the photon density is much higher than in ordinary continuous-wave (CW) lasing. This high photon density supports and is supported by a high level of stimulated emission. The result is that the inversion is reduced very quickly to a level far below that at which it started. This means that Q-switching can extract energy from the lasing medium much more efficiently than CW lasing can, making it useful any time a high intensity of light is desired.

There are many different physical means of achieving the change in cavity loss required for Q-switching. The methods which have been used include spinning or vibrating mirrors, electrooptic effects such as the Pockels effect in crystals and the Kerr effect in liquids, acoustooptic effects in crystals, and saturable absorbing dyes. The latter are solutions of complex organic molecules which have a high absorption coefficient if the intensity of light is low, but which "bleach" and become transparent at high intensities.

2.4.2 Q-Switched Pulse Characteristics

Wagner and Lengyel [8] found that by assuming that the change in cavity loss took place very quickly, and neglecting slow processes such as pumping and spontaneous emission during the buildup of the Q-switched pulse, they were able to describe the buildup of the pulse with a pair of differential equations. In my notation, these are:

$$\begin{aligned}\frac{d\phi}{d\tau} &= \phi \left(\frac{n_l}{n_t} - 1 \right) \\ \frac{dn_l}{d\tau} &= -\phi \left(\frac{2n_l}{n_t} \right)\end{aligned}\tag{2.9}$$

where ϕ is the total number of photons in the cavity,

n_i is the total inversion in the lasing medium,

τ is the time from Q-switching, in units of t_c ,

and n_t is the total threshold inversion.

The first of these equations expresses the fact that each stimulated emission increases the number of photons in the cavity by one, and that on average one photon leaves the cavity every t_c seconds due to the cavity loss, \mathcal{L} . The second equation expresses the fact that for each photon created by stimulated emission, the total inversion of the lasing medium decreases by two. This is because an electron moves from the upper laser level to the lower laser level, and the lifetime of the lower laser level is long compared to the risetime of the Q-switched pulse, even in a four-level laser.

Wagner and Lengyel were able to solve this system of equations and find an expression for the amount of energy released by stimulated emission:

$$\mathcal{E} \approx \frac{n_i h \nu}{2}, \quad \text{for } n_i \gg n_t \quad (2.10)$$

where n_i is the total initial inversion in the lasing medium,

h is Planck's constant,

and ν is the frequency of the radiation.

The total threshold inversion is given by the formula

$$n_t = \frac{8\pi n^2 t_{spont} \Delta \nu V}{\lambda^2 c t_c} \quad (2.11)$$

where n is the index of refraction of the medium,

t_{spont} is the radiative lifetime of the lasing medium,

$\Delta\nu$ is the width of the spontaneous fluorescence spectrum,
and V is the volume of lasing material present.

The fact that the energy given by equation (2.10) does not depend on the cavity losses is due to the assumption that the threshold inversion can be ignored relative to the initial inversion, since under these conditions the Q-switched pulse will build up rapidly, and so the effect of cavity losses can be ignored during the time when energy is being released by stimulated emission.

Koechner [2] uses Wagner and Lengyel's approach to produce an expression for the duration of the Q-switched pulse:

$$\Delta t_p \approx t_c \frac{n_i - n_f}{n_i - n_t [1 + \ln(n_i/n_t)]} \quad (2.12)$$

where n_f is the total inversion left after lasing is complete.

For large n_i , Δt_p will be only slightly longer than t_c .

2.5 Cavity Dumping

The technique of *cavity dumping* is a way of getting energy out of a laser more efficiently than the usual method, which is to make one of the end mirrors partially transmitting so that light leaks through to be used as the laser's output. In a cavity-dumped laser, both mirrors are as close to 100% reflective as possible, and an electrooptic or acoustooptic device is used to "switch" the light out of the cavity when its intensity reaches a maximum. This technique can be used alone on a CW laser, or can be combined with Q-switching to produce shorter, more symmetrical, pulses than would be produced by the latter

technique alone. The combination of cavity dumping and Q-switching is frequently referred to as "pulse transmission mode" (PTM) Q-switching [9].

If the device used to switch light out of the cavity changes state in a time much shorter than the cavity round-trip time and introduces a loss near 100% to the cavity, then the width of the resulting output pulse will be close to the round-trip time of the cavity. This occurs because in one round-trip time, all the light which was in the cavity prior to the time of switching passes the switching device and is deflected out of the cavity. If the laser is both Q-switched and cavity-dumped (PTM), the energy of the output pulse will be approximately the same as that which would have been obtained from an equivalent laser which is only Q-switched [10]. Its energy will thus be given by equation (2.10).

The reason why a PTM laser produces a pulse with the same amount of energy as an equivalent Q-switched laser's is that when either laser's Q-switch triggers, light energy builds up very rapidly in the cavity, so that much of the stimulated emission takes place early in the Q-switched pulse's development. In the non-cavity-dumped case, this energy then decays relatively slowly by transmission through the output mirror. During this stage, there is still a small amount of stimulated emission occurring, but it does not add a significant amount of energy to the light in the cavity. In the PTM case, the peak energy in the cavity is rapidly removed by the switching device, producing a pulse which is shorter, but which does not have significantly less energy.

Since the energies in the two types of pulse are essentially the same, while the cavity-dumped pulse's length is generally several times shorter (assuming a reasonable output coupling loss for the non-dumped case), it is clear that the intensity of the light produced by

a PTM system is generally higher than that from an equivalent Q-switched system without cavity dumping.

The next chapter describes the design and development of a laser system which combines the short pulse length and high intensity of a pulse transmission mode system with the high gain and small beam divergence of an unstable-resonator YAG laser. The expected performance of the laser is estimated using the formulas from the present chapter.

Chapter 3

System Development

3.1 Introduction

The design of the Nd:YAG laser system was changed several times over the course of this thesis project, to correct problems that were discovered and to improve performance. This chapter describes the initial design and performance estimates for the laser, the tests that were run on it, and the design changes that were made as a result of those tests.

3.2 Initial Design

3.2.1 Optical Components

The initial design for the Nd:YAG laser described in this thesis was based on the design of the ruby laser it is to replace [11]. It used two Pockels cell/polarizer pairs to introduce controlled losses to the cavity: one for Q-switching, and one for cavity dumping. A schematic of the original layout of the YAG laser is shown in Figure 3.1.

As shown, the resonator is composed of two mirrors, labelled M_1 and M_2 . M_1 is 2.2 cm in diameter and is concave with a radius of curvature of 10 m. M_2 is the same size, but is convex with a radius of curvature of 7 m. Both mirrors are high-reflectivity dielectric laser mirrors. The initial perpendicular separation of the mirrors was 1.58 m, which was

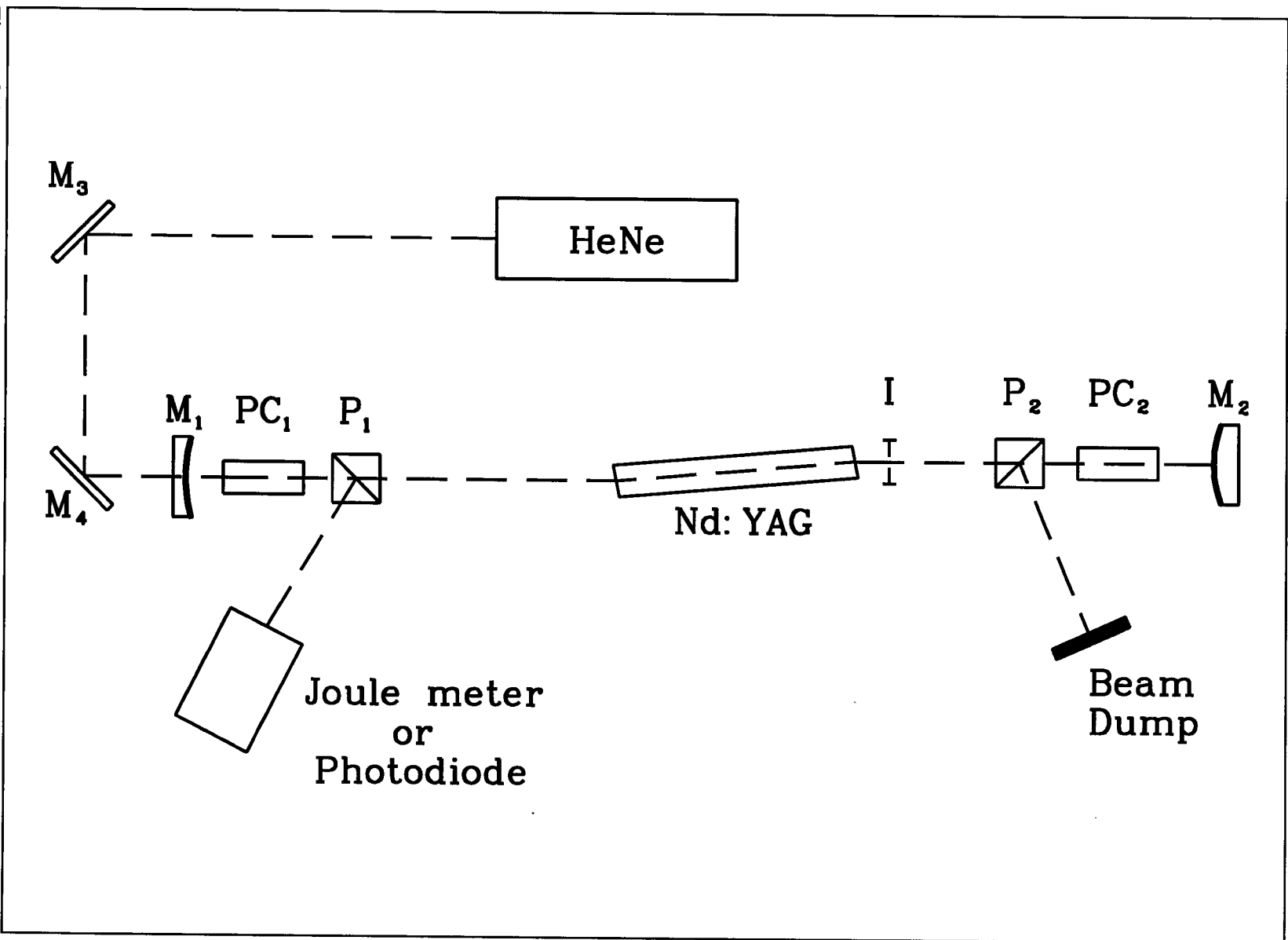


Figure 3.1: Schematic diagram of the initial YAG laser cavity layout.

chosen to make the effective length of the cavity for purposes of geometric ray tracing* equal to 1.5 m, so that the mirrors would be confocal. The round-trip time of light in the cavity was 11.6 ns.

The Nd:YAG laser rod is circular in cross-section, with a diameter of 6.35 mm and a length of 10 cm. The ends of the rod are antireflection coated (1.064 μm) and are parallel, with a wedge angle of 6° from normal. The doping level is high, with 1.1% of the yttrium atoms in the crystal having been displaced by neodymium atoms. For efficient pumping of the rod, it is mounted in a metal reflector whose cross-section has the form of two overlapping ellipses, with one focus of each coinciding. The rod is located at that focus, and a xenon flashtube is located at each of the other two foci, so that the light from the flashtubes is focused into the rod. The rod is cooled by a continuous flow of room-temperature water over its surface, and the flashtubes are cooled by air flowing through their mounting tubes.

The Pockels cells, PC_1 and PC_2 , are both 9 x 9 x 25 mm lithium niobate (LiNbO_3) crystals. Each is cut such that the optical axis lies along the length of the crystal. The end faces have an anti-reflective coating, which is optimized for 1.064 μm . One pair of opposing faces perpendicular to the beam path have gold electrodes deposited on them. The theoretical DC quarter-wave voltage for these crystals is 1 514 V at 1.064 μm .

The polarizers, P_1 and P_2 , are of the standard Glan-Foucault type, and are oriented such that the horizontal polarization is transmitted and the vertical polarization is deflected

* The effective length referred to here is not the optical path length, which is of course longer than the physical length of the cavity. This distinction should be familiar to the reader: a stick appears to get shorter when it is stuck into a bucket of water, despite the fact that the optical path length to its end has increased. (I am indebted to H. Houtman for this analogy.)

out of the cavity. Because their faces are not antireflection-coated, the polarizers were angled slightly to prevent the formation of sub-cavities.

In addition to the above components, an iris, labelled "I" in the diagram, was introduced to the cavity to limit the diameter of the propagating modes of light to less than the diameter of the laser rod, so as to prevent light from scattering off of its unpolished sides. This is formally equivalent to reducing the sizes of both end mirrors, and so to first order it introduces no additional loss to the cavity, as discussed in section 2.3.2. With the iris in place, however, essentially all of the unstable resonator loss is "due" to light being intercepted by it. The amount of light intercepted is sufficiently large that the intensity in the cavity was monitored by tilting the iris at a slight angle and attaching an annular aluminum reflector to it, to deflect light towards a nearby high-speed photodiode. This was omitted for clarity in the figure above, but is shown in Figure 3.5.

Because the mirrors M_1 and M_2 are partially transparent to visible light, the laser could be aligned by running the beam from the helium-neon (HeNe) laser through the back of M_1 and down the length of the cavity with the aid of plane mirrors M_3 and M_4 . The reflection from M_2 was large enough that the reflected pulse could be traced back to P_1 to ensure that the Pockels cells and mirrors were oriented normal to the beam. A removable aperture was placed between P_1 and the YAG rod during alignment to aid in detection of the reflected spot.

3.2.2 Flashtube Pumping

As already mentioned, the initial inversion in the YAG rod is produced by a flash of light from two xenon flashtubes. The tubes chosen have an arc length of 3", a bore diameter of 9 mm, and a rated maximum energy per flash of 600 J. Their operating voltage range is from 1.5 kV to 2.5 kV.

Flashtube lifetime is characterized by the ratio of the energy of the applied voltage pulse to the tube's "ultimate limit": the maximum energy the tube can handle without shattering [12]. The ultimate limit is given, in Joules, by the empirical formula

$$U_{lim} = 90 LD\sqrt{T} \quad (3.1)$$

where L is the arc length, in inches,

D is the bore diameter of the tube, in mm,

and T is the flash duration, in ms.

The units used for L and D in this equation were chosen to match the units used by EG&G in the specifications for the flashtubes they manufacture. It seems odd, but their tubes have bore diameters which are integral in millimetres, and arc lengths which are integral or half-integral in inches. I presume that this is due to a preference for specifications in inches being frustrated by quartz tubing only being available in metric diameters.

A flash duration of 43.5 μ s was chosen to make the pumping time much less than the lifetime of the upper laser level, so that there would be little loss due to spontaneous fluorescence and nonradiative decays. Substituting this into the equation gives $U_{lim} = 507$ J. The manufacturer's recommendation for a flashtube enclosed in a reflective cavity, as is the case here, is for the flash energy not to exceed 40% of U_{lim} , because the large amount of light returned to the tube by the reflector increases the tube's thermal stress.

The energy for the flash comes from two two-stage pulse-forming networks, which have characteristic impedances of about 0.3 Ω —to roughly match the resistance of the flashtube arcs—and total capacitances of about 71.6 μ F. These produce simultaneous 43.5 μ s

long current pulses in each tube, with an energy given by $0.5 CV^2$, where V is the initial charging voltage of the networks.

The voltage on the networks is limited at the low end by the minimum operating voltage of the flashtubes, and at the high end by the thermal stress considerations discussed above. This results in an operating voltage range of 1.5 kV to 2.38 kV, or an energy range of 80 J to 203 J per pulse. To minimize tube wear, and to allow room to compensate for deterioration of the flashtubes with age, the charging voltage used for most firings of the laser was in the neighbourhood of 1.74 kV, which corresponds to a pump energy of about 110 J. According to reference 12, this should result in a tube lifetime of better than 1 000 shots.

3.2.3 Timing and Triggering

Once the pulse-forming networks are charged, the laser is triggered by a push button connected to a two-channel electronic delay unit, located in an electromagnetically-screened room. This unit produces two 40 V output pulses at times which can be set independently in intervals of 100 ns. The first pulse, at $t = 0$, goes to a silicon-controlled rectifier unit which produces a short 400 V pulse. This pulse is stepped up to 20 kV by a transformer, and is applied to the metal reflector surrounding the YAG rod and the flashtubes. The high electric field caused by this pulse makes the gas in the flashtubes break down, and current is supplied to them by the pulse-forming networks described above.

Near the end of the flashtube pulse, the second channel of the delay unit triggers, sending a 40 V pulse to a krytron unit which produces a 23 ns long, 5 kV output pulse, which is used to trigger the ultraviolet-triggered spark gap which controls the two Pockels cells. When the laser system is used as a diagnostic with the 12 J CO₂ laser, this krytron unit

will no longer be necessary, as the spark gap will be triggered directly by the trigger pulse that comes out of the CO₂ laser's spark gaps.

A schematic diagram of the initial design for the Pockels cell triggering circuitry is shown in Figure 3.2. This design was based on that of the circuit used in the existing ruby laser. Until the gap is triggered, coaxial cables L₁ and L₂ are held at the quarter-wave voltage of the cell, $V_{1/4}$, which means that PC₂ is at $V_{1/4}$, while PC₁ is at 0 V. The cavity is thus in a high-loss situation, because of the voltage on PC₂. When the spark gap is triggered by the application of a high-voltage pulse to its trigger pins at time t_g , it becomes conductive, allowing the voltage in the charged cables to flow through into cables L₃ and L₄. A decreasing step pulse propagates back up cables L₁ and L₂ towards their ends. This pulse reaches PC₂ at time $t_g + 3l_1/(2c)$, where l_1 is the length of cable L₁. This causes the voltage across PC₂ to drop rapidly to 0 V, which means that the loss in the cavity should drop to its diffraction-limited value, allowing light to begin to build up via stimulated emission. At time $t_g + 3l_3/(2c)$, the voltage pulse in cable L₃ reaches PC₁, causing the voltage across it to rapidly rise to $V_{1/4}$, which causes the light in the cavity to be dumped out of polarizer P₁. The length of cable L₃ is chosen such that this occurs when the intensity of the light in the cavity reaches its peak.

The length of time for which the cavity-dumping pulse is applied to PC₁ is controlled by the length of cable L₂. Specifically, the duration of the dump signal will be given by $3l_2/c$. This was initially chosen to equal 6 ns, the desired output pulse length.

The 4 Ω resistor and 10 nF capacitor wired in parallel to the gap help maintain the discharge and ensure that the initial current is high—over 300 A. This decreases the

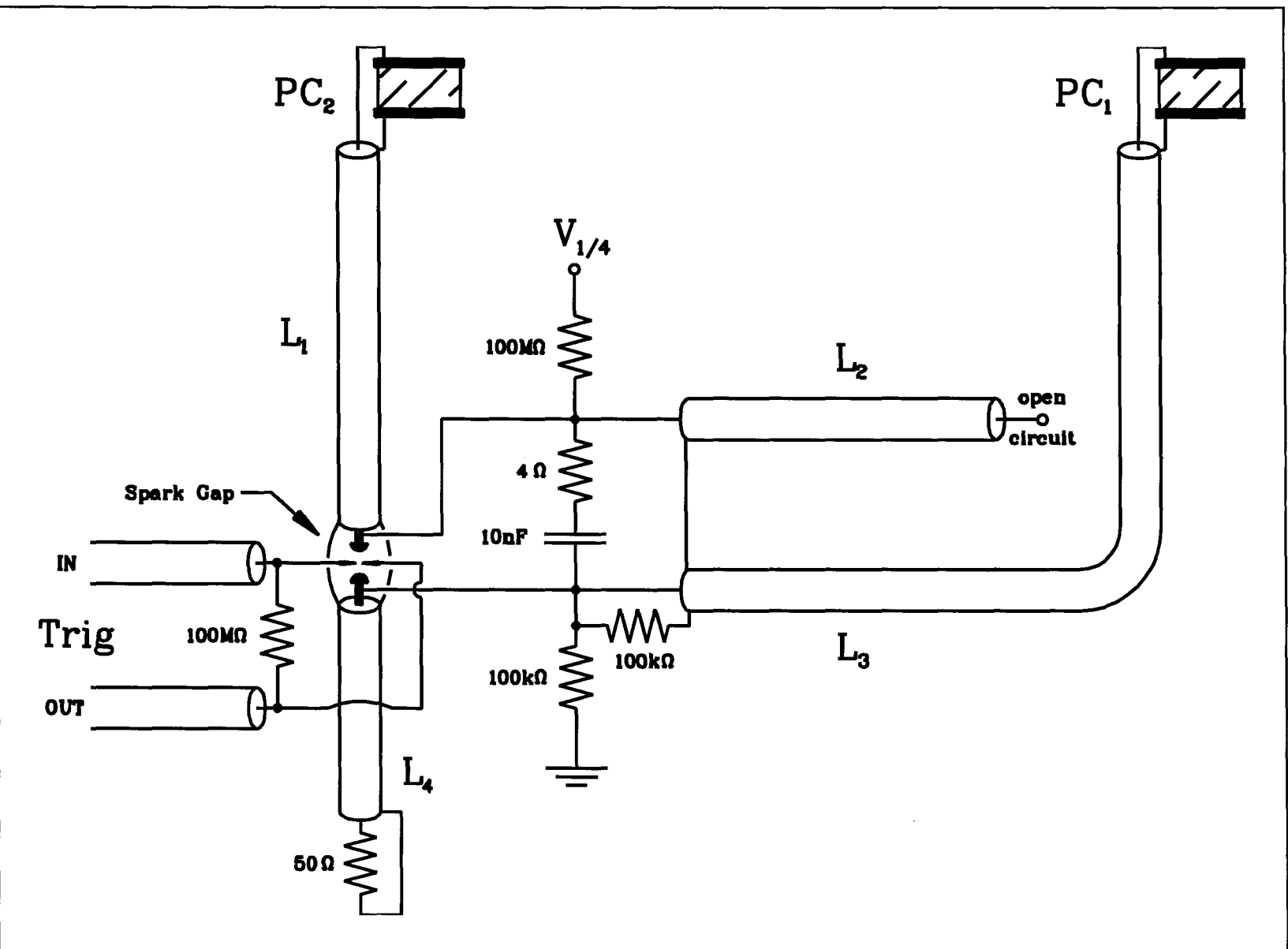


Figure 3.2: Schematic of the initial Pockels cell triggering circuit design.

resistance of the gap, allowing the voltage step pulses to pass through with less distortion of their shape.

3.2.4 Expected Performance

The expected performance of the laser can be estimated by using the formulas given in Chapter 2 and the component specifications given in section 3.2.1. While the estimates obtainable will not be extremely precise due to the need to make some assumptions along the way, they will illustrate the general performance to be expected from the laser.

Substituting the appropriate values into equation (2.3) shows that the diffraction loss in the YAG laser's cavity should be approximately 0.29 per pass. The loss due to transmission through the mirrors will be negligible, so the only other losses are those due to scattering off of components (particularly the polarizers, which are not antireflection-coated), and due to absorption in the YAG rod and other parts. All of these losses can be included in the distributed loss constant, α , in equation (2.4). A reasonable approximation for these is to take $\mathcal{L}_{nd} \sim 0.05$. Substituting \mathcal{L}_{nd} and \mathcal{L}_{diff} into equation (2.5) gives $\mathcal{L} \approx 0.33$.

Putting the above loss per pass into equation (2.8), the photon lifetime in the cavity is calculated to be about 18 ns.

The total threshold inversion of the laser is given by equation (2.11). The index of refraction, n , of Nd:YAG is 1.82 in the vicinity of 1 μm . The width of the spontaneous fluorescence spectrum of YAG, $\Delta\nu$, is about 1.8×10^{11} Hz. Substituting these values into the equation gives a threshold inversion of 4.4×10^{15} .

In order to calculate the pulse energy and other parameters, the initial inversion of the laser is also needed. Because the duration of the flashtube pulse is much less than the

spontaneous fluorescence lifetime of the YAG rod's upper laser level, the total initial inversion can be estimated by using the formula

$$n_i \approx \frac{U_{lamp}}{h\nu_{laser}} \cdot e \quad (3.2)$$

where U_{lamp} is the energy of the electrical pulse applied to the flashtubes,

and e characterizes the efficiency of energy transfer from the electrical pulse through to the electrons in the upper laser level.

Following Yariv [3], the efficiency with which the flashtubes convert electrical energy into light can be roughly estimated to be about 0.5. About 5% of the light will fall within the absorption bands of the YAG crystal, and only about 5% of that will actually be absorbed. Finally, when an electron decays from the absorption bands to the upper laser level it loses energy, which must be accounted for within e . The fraction of energy remaining after this decay will be roughly equal to $\nu_{laser}/\nu_{lamp} \sim 0.5$. Combining these factors gives a value for e of about 6.25×10^{-4} .

Assuming a lamp energy of 110 J and the above value for e , equation (3.2) gives $n_i \approx 3.7 \times 10^{17}$. The ratio of initial to threshold inversion is thus $n_i/n_t \approx 85 \gg 1$, therefore equation (2.10) can be used to estimate the energy of the Q-switched and cavity-dumped pulse. Substituting the above results into the equation gives a pulse energy of about 35 mJ. While this is a bit less than the goal for this laser, it is not a major problem, as it was expected that an amplification stage would need to be added before the laser could be used to replace the existing ruby laser (which also used an amplifier to boost its output energy).

Because $n_i \gg n_r$, it follows that $n_i \gg n_f$, so equation (2.12) can be used to calculate the width of the Q-switched pulse in the laser when cavity dumping is disabled. The resulting width is about 19 ns, only a little longer than t_c .

3.3 Tests and Design Modifications

3.3.1 Preliminary Tests

The first test made during construction of the laser was that the flashtube pulse was of the correct length. This was determined by measuring the current passing through the tubes by means of a Rogowski coil wrapped around their ground leads. The full width at half-maximum (FWHM) of the current pulse was $50 \pm 4 \mu\text{s}$, which is reasonably close to the expected value of $43.5 \mu\text{s}$. A measurement taken much later, after the tubes had been fired hundreds of times, gave a pulse width of $44 \pm 4 \mu\text{s}$, with a slightly less square pulse shape. This change in the shape and duration of the pulse may be due to erosion of the flashtube electrodes, although no other deterioration in performance has been noted.

A great deal of time was spent constructing and adjusting the spark gap to control the Pockels cell timing. The design chosen, like that of the timing circuit as a whole, was based on that used in the existing ruby laser. This proved to be less than ideal, as the ruby laser used KDP * Pockels cells, which have a much higher quarter-wave voltage than the LiNbO_3 cells used with the YAG laser. Because the voltage being switched was many times smaller, the electrodes in the spark gap had to be much closer together in order for them to break down properly. This caused problems because the thread of the screws used to adjust the

* KDP is an abbreviation for "potassium dihydrogen phosphate", KH_2PO_4 .

electrode separation was too coarse to allow accurate adjustment of such a small gap. The small electrode separation also caused great problems in triggering the gap, because the small gap and relatively large electrode diameter made it difficult to get enough ultraviolet light from the trigger pins into the gap to break it down.

Because of these problems, it took a fair bit of effort to get the gap adjusted so that it would trigger reliably, and it required readjustment more frequently than would be desired in a working laser system. No attempt was made to accurately measure the jitter of the gap, because it was apparent that a new spark gap or other suitable triggering device would have to be constructed before the laser could be incorporated into the experimental system. Jitter in the spark gap's triggering was not a problem for purposes of testing the laser, as the timing circuitry always maintains a fixed delay between Q-switching and cavity-dumping, regardless of spark gap jitter. The length of the delay between the flashtube pulse and the triggering of the Q-switch only needs to be accurate to within a few microseconds, so spark gap jitter causes no problem there either.

Once the spark gap was triggering reliably enough to run tests, its performance was studied by connecting cable L_3 , which would normally go to the cavity-dumping Pockels cell, to an oscilloscope via a series of attenuators. The initial results were far from the ideal 1514 V square pulse. This problem turned out to be due to the connectors used to join the cables to the Pockels cells not being able to handle the voltage needed, and due to attenuation in the cables. Replacing the wiring with thicker coaxial cable and using high-voltage connectors solved both problems, resulting in a 7 ns FWHM pulse with the correct amplitude. The shape of the pulse was still a problem, however, as it had a risetime of 4 ns, and a similar decay time.

Before any attempt was made to solve the cavity dumping voltage pulse shape problem, the laser was tested out with cavity dumping disabled. The light intensity in the cavity was monitored by means of a PIN photodiode aimed at the intra-cavity iris, and Q-switched pulses with FWHMs of 30 ± 4 ns were observed to occur 60 ± 4 ns after the spark gap was triggered. The pump energy was varied from 106 J to 155 J and no significant change in the Q-switched pulse build-up time was observed.

The variation in the height of the Q-switched pulse was also studied as a function of the delay between the firing of the flashtubes and the triggering of the spark gap. As expected, if the delay was less than about 40 μ s the intensity of the Q-switched pulse was greatly reduced, because the gap was then firing before the flashtubes had finished pumping the YAG rod. For delays between 40 μ s and 80 μ s, the intensity was relatively insensitive to the exact length of the delay, because these times are much shorter than the lifetime of the upper laser level. The delay setting chosen for permanent use was 75 μ s.

It was decided that because of the relatively long risetime of the cavity dumping voltage pulse, the length of the pulse should be increased from a nominal value of 6 ns to 12 ns, in order to have a longer period of constant voltage on the Pockels cell. A second reason for this change was that it was realized that the cavity round-trip time was fixed at 11.6 ns by the requirement that the mirrors be confocal, and having a cavity-dumping time that is less than the cavity's round-trip time would be inefficient, as only part of the energy in the cavity would be dumped.

Finally, cavity dumping was enabled, and output pulses with a FWHM of 12 ± 4 ns were observed. There was a significant variation in the height of the pulses from shot to shot, which was attributed to the lack of longitudinal mode control in the laser cavity. In the

existing ruby laser, this problem was solved by the introduction of a Fabry-Perot etalon. This solution cannot be applied to the YAG laser because it does not use planar mirrors, so the etalon would distort the curvature of the modes in the cavity, ruining the collimation of the laser's output.

The energies of the output pulses were measured with a GenTec Joule meter, and were found to vary from 0.15 mJ to 3.6 mJ—far below what was expected.

3.3.2 Optimization of Output

By means of various improvements to the alignment of the cavity, the energy range of the output pulses was increased to 6 - 10 mJ. The light in the cavity was monitored with and without cavity dump, and there was not much difference between the two. It was clear that no more than 10 - 15% of the light in the cavity was being dumped. The timing of the dump signal was checked and appeared to be fine.

The energy output was studied as the Pockels cell voltage was varied, and the results are shown in Figure 3.3. Despite the fact that an average of several shots was used at each value of voltage, there are four anomalously low points on the graph. These seem to represent temporary reductions in the laser's output, and may be due to thermal lensing and birefringence in the rod due to a buildup of heat when many shots were taken in succession. Their occurrence was not generally repeatable. The curve shown on the graph is a weighted least-squares fit to the data, excluding the four anomalous points. The peak energy output seemed to occur for Pockels cell voltages between 1.8 and 1.9 kV, which is significantly higher than the theoretical value, 1.514 kV.

Measurements using the helium-neon alignment laser showed that the DC quarter-wave voltage for the HeNe's 632.8 nm beam was also higher than its theoretical value, and

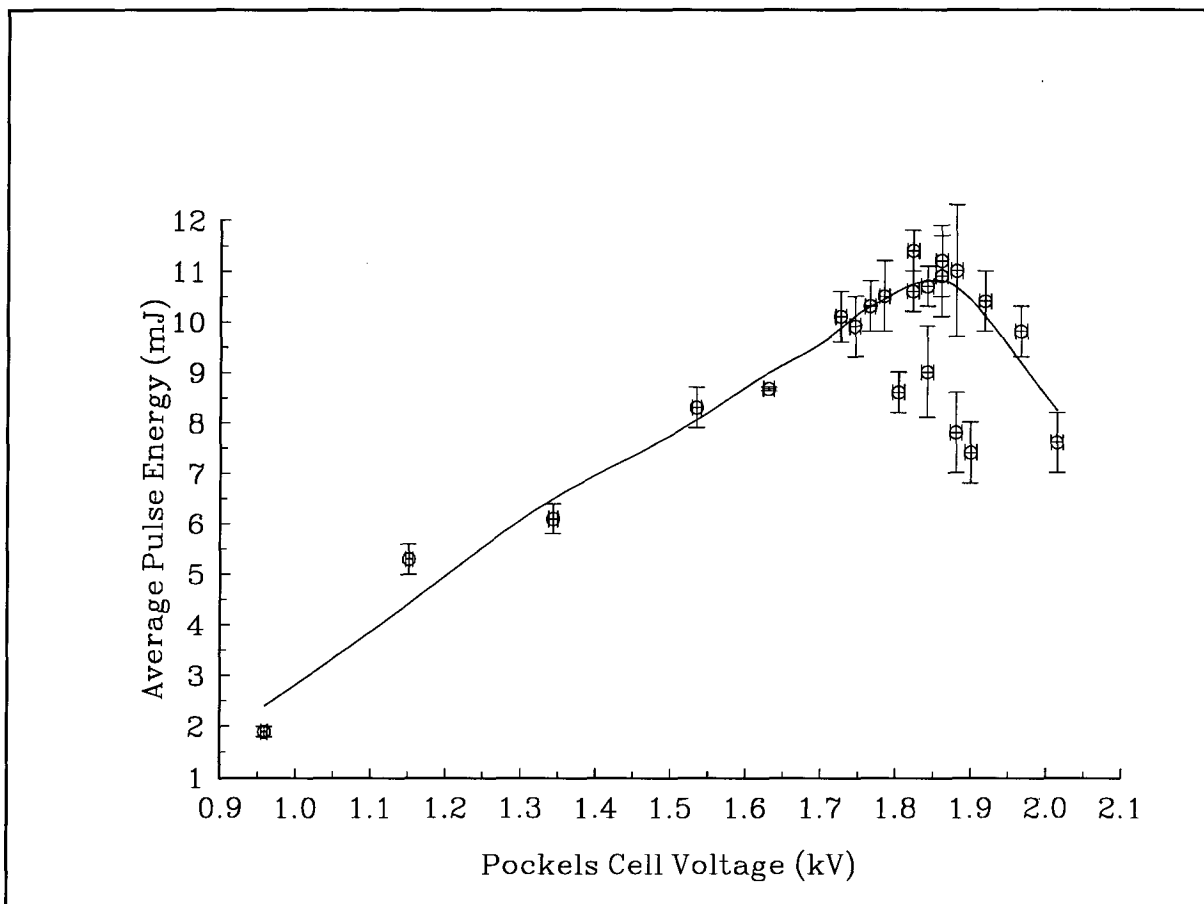


Figure 3.3: Variation of cavity-dumped output energy with Pockels cell voltage. Each point is an average of 5 shots. The curve is a weighted least-squares fit to the data, excluding the four anomalously low points.

by the same amount, once the effects of the frequency difference were taken into account. This effect seems to represent some problem with the crystal itself.

The Pockels cell voltage setting chosen for future use was 1.822 kV, as this seemed more or less optimum. Generally pulses in the 10 - 11 mJ range were produced. With certain mirror alignments, pulses as large as 16 mJ could be obtained, but the shot-to-shot energy stability was drastically reduced.

The variation in the laser's output energy was also studied as the pump energy was varied from 99 J to 180 J, and no significant increase was observed. This result was somewhat unexpected, as the amount of energy released should increase with greater pump energy, unless the inversion in the rod is saturated. Based on the estimates of section 3.2.4, pump energies in the range studied should only be sufficient to excite electrons to the upper laser level in 1% - 2% of the Nd atoms in the crystal.

In the course of studying this strange behaviour, it was discovered that when the laser was fired, 130 - 170 mJ of energy came out of the Q-switch polarizer. When cavity dumping was disabled, this energy increased to 175 - 185 mJ. Photodiode measurements showed a strong pulse of the same general shape as the previously-observed intracavity light, coming out of the polarizer at about the same time as light builds up in the cavity. This indicated that the Pockels cell/polarizer combination was not producing zero loss after triggering, contrary to expectations, and also suggested that the cavity-dumping cell and polarizer were not introducing 100% loss, because otherwise a greater fraction of the light in the cavity would be coming out of the cavity-dump polarizer.

As this problem with the Pockels cells was clearly causing the loss of the majority of the energy produced by the laser, efforts from this point on focused on finding the cause of this problem and fixing it. These efforts are discussed in the next section.

3.3.3 Attempts to Diagnose and Correct the Pockels Cell Problem

The first test performed on the Q-switch cell was to run the beam from the helium-neon laser through it and see how much light was deflected out of the cavity as a function of Pockels cell voltage. Because of the geometry of the cavity, the cell was between parallel polarizers, as shown in Figure 3.1. This test indicated that the cell had an extinction ratio* of 50 ± 20 , which seems rather low. Koechner [2] mentions that an ordinary extinction ratio for a Pockels cell in a laser system is "a few hundred".

The effect on extinction of the pressure of the clamps holding the LiNbO_3 crystals in place was investigated, because Koechner states that clamping can introduce some birefringence in these crystals. It was found that reducing the clamp pressure did improve the extinction ratio slightly, but this caused no improvement in the laser's performance.

The alignment of the polarizers was also improved, to make certain that their axes of polarization were accurately parallel to one another. This improved the extinction ratio to 230 ± 110 , but caused no real improvement in the laser's performance.

Next, the voltage pulses being applied to the Pockels cells were examined. Attempts were made to measure the pulses by various direct and indirect means, but no way of doing so was found which would allow measurement on a fast enough timescale to be useful

* The *extinction ratio* for a Pockels cell is normally determined by placing the cell between crossed polarizers, and finding the ratio of the maximum to the minimum transmitted light intensity as the voltage is varied from zero to $V_{\lambda/2}$. This is slightly different from the test conditions described above, but the results should be equivalent.

without altering the shape of the voltage pulses being measured. Attention was then focused on improving the shape of the cavity-dumping electrical signal, as viewed by connecting the cable that normally goes to the cavity-dumping cell to a scope via an attenuator.

As already mentioned, the shape of this pulse was not particularly square. It was improved by simplifying the switching circuitry so that the electrical signal used for cavity dumping came directly from the charged cable connected to the Q-switch cell, as shown in Figure 3.4. This simplified the circuit and improved the impedance matching at the spark gap. The resulting electrical signal was a very nice square pulse with an amplitude of 880 ± 50 V, a FWHM of 12.2 ± 0.4 ns, and a risetime of 1.6 ± 0.4 ns, indicating that the voltage on the Q-switch cell had to be dropping all the way to zero in a similar amount of time. This resulted in a slight improvement in the laser's performance. In combination with an improvement in the positioning of the cavity-dump polarizer, the above change increased the typical output energy of the laser to 18 ± 2 mJ. On occasion, pulses with energies as high as 23 mJ were observed. There was still approximately 120 mJ coming out of the Q-switch polarizer on each shot, however, indicating that the pulse shape had not been the root cause of the problem.

Another suspected cause was that there might be some sort of self-focusing effect occurring in the Q-switch cell due to the beam having a relatively narrow diameter there (it being closer to the convex mirror than the other cell, as shown in Figure 3.1). To see if this was the cause of the problem, the wiring to the two Pockels cells was reversed, so that the cell which had formerly been the cavity-dump cell now became the Q-switch cell, and vice versa. No significant improvement in performance was observed, and lasing became somewhat erratic, so this approach was abandoned.

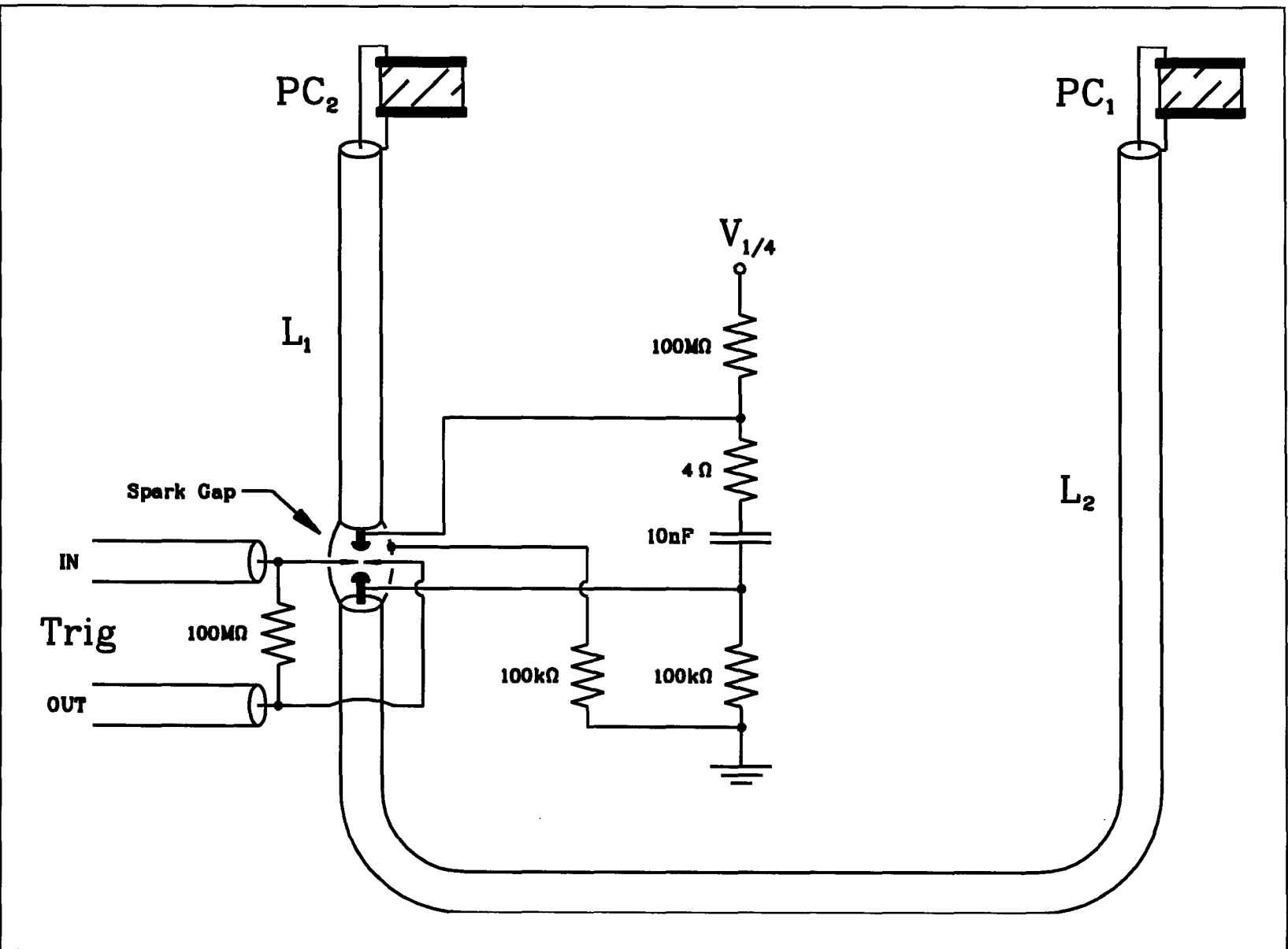


Figure 3.4: Schematic of Pockels cell control circuit with simplified cavity dump system.

Some problems with poor Q-switch performance using KD*P[†] Pockels cells have been reported to be caused by fast switching of the voltage on the cell inducing an acoustic wave in it [13]. This interferes with proper Q-switching because the electrooptic coefficients change locally when there is stress on part of the crystal. An attempt was made to see if increasing the risetime of the pulses on the YAG's Pockels cells had any effect by wiring capacitors of various sizes across them, to increase the risetime and decay time of the voltage pulses. This made the laser very unreliable and produced no improvement in output energy.

Finally, it was decided to simplify the laser by using a single Pockels cell and polarizer to both Q-switch and cavity dump the system. A schematic of the resulting layout and triggering circuitry is shown in Figure 3.5. This change simplifies alignment of the cavity and reduces losses, because the laser contains fewer optical components. Because of the removal of components, the mirror separation was decreased to 1.56 m, which resulted in a round-trip time for light in the cavity of 11.2 ns. These changes do not significantly alter the results of section 3.2.4.

The triggering circuit used with this configuration is the same as that shown in Figure 3.4, except that the cable which formerly went to Pockels cell 1 is now left unterminated, so that the voltage pulse which formerly went to PC₁ is now reflected back to PC₂. The lengths of the cables were adjusted to ensure that this pulse would arrive at PC₂ at the appropriate time for cavity dumping.

No significant change in the performance of the laser was observed as a result of the removal of the Pockels cell, but the change did result in a major decrease in the amount of electrical noise being picked up by the PIN photodiodes used to measure the light in the

[†] KD*P is the standard abbreviation for deuterated potassium dihydrogen phosphate.

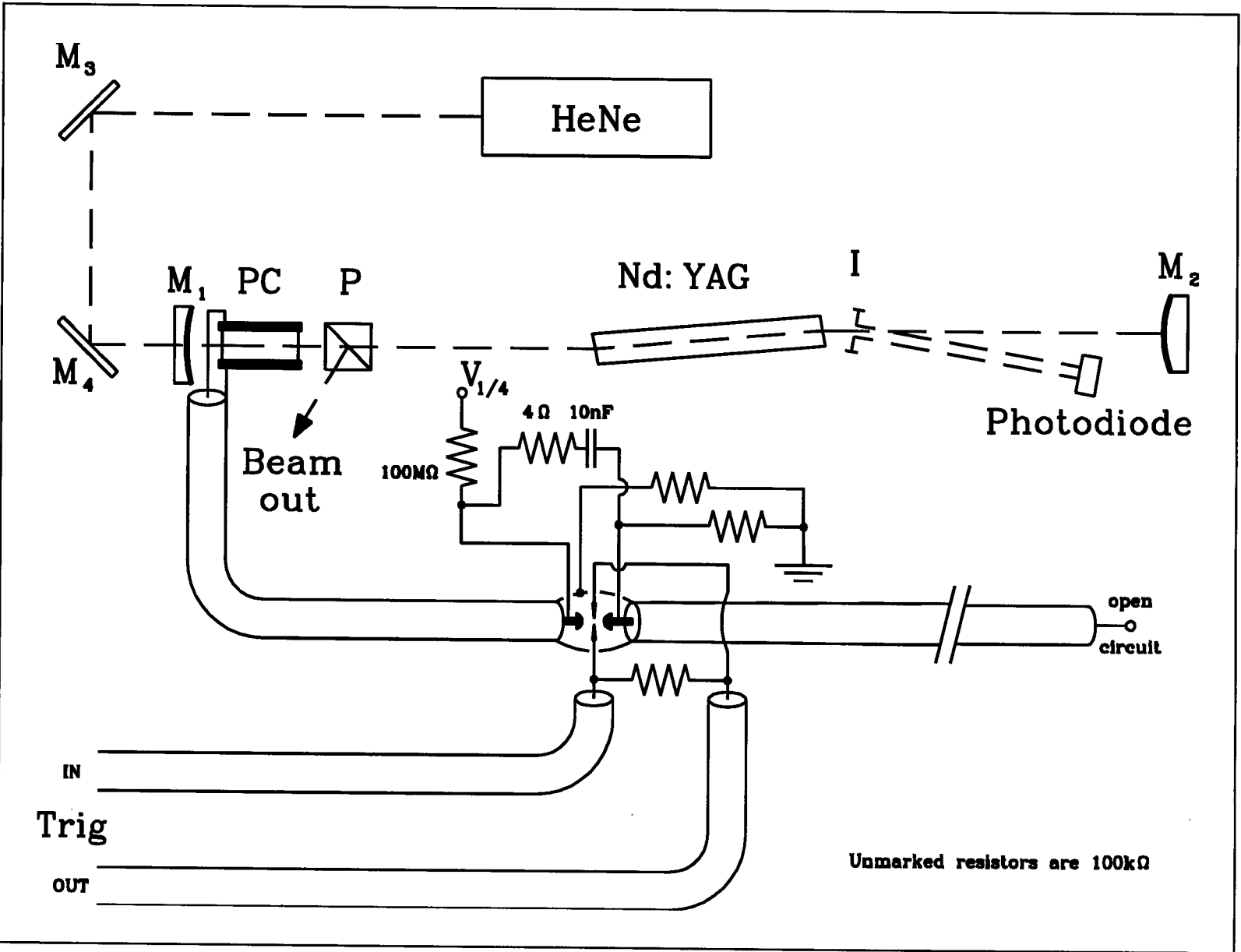


Figure 3.5: Schematic diagram of final YAG laser cavity layout, with Pockels cell control circuit.

cavity and the light coming out of the polarizer, since there was now less high-voltage wiring near them. This made visible something which had not been seen previously: a series of low-intensity pulses of light in the laser beginning about 35 μs before the Pockels cell was triggered. When the light in these prelasing pulses was integrated with a simple RC circuit, it was found that they were taking up the majority of the energy from the laser rod, as shown in Figure 3.6.

Some notes on the figure are in order. The traces begin at the firing of the flashtubes. The spike which extends off-scale about 75 μs later is the Q-switched light in the cavity. It is an order of magnitude larger in intensity than the prelasing pulses. The integrated trace shows that the energy in the Q-switched pulse was no more than 20% of the total energy extracted from the YAG rod. This figure is comparable to the ratio of the difference in energy coming out of the Q-switch polarizer with and without cavity dumping to the energy that comes out without dumping (see p. 35). It should be noted that while the RC time of the integrator used is clearly not quite long enough for accurate integration, the trace produced still provides an upper bound on the ratio of the energy of the Q-switched pulse to the total energy extracted, which is sufficient for diagnostic purposes.

Clearly, what was happening in the laser was that the Pockels cell, even when held at its quarter-wave voltage, was not introducing sufficient loss to the cavity to hold off lasing. As a test, the beam path was blocked by placing a piece of white cardboard in the cavity. If the cardboard was placed anywhere but between the concave mirror and the Pockels cell, no lasing took place. If it was placed in the latter location, a small amount of prelasing was observed, beginning about 20 μs before the Q-switch was triggered. This indicates that even the small amount of reflection from the Pockels cell's antireflection-coated end faces is

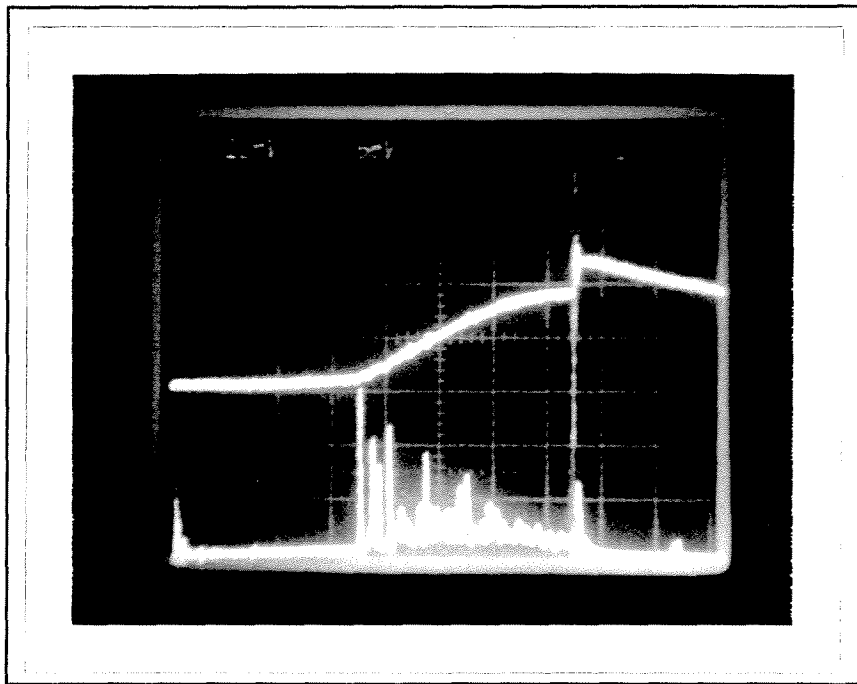


Figure 3.6: Light in the laser cavity (lower trace) and its integral (upper trace). Horizontal scale is $10 \mu\text{s}/\text{division}$. Vertical scales are arbitrary.

sufficient to cause prelasing, due to the high gain of the YAG rod. This prelasing, however, was negligible compared to that without the cardboard, indicating that the main problem was that the Pockels cell was not producing enough loss, rather than that the reflection from its faces was too large.

This problem with prelasing is reported by Koechner [2] to be extremely common with YAG lasers, due to the high gain of the Nd:YAG lasing medium.

An attempt was made to decrease the effect of this prelasing by decreasing the length of the delay between the flashtubes firing and the Q-switch being triggered. This was not found to be useful, as decreasing the delay led to postlasing because the Pockels cell was being switched before the flashtubes had finished pumping the rod, so that a lot of energy was left in the cavity after the Q-switched pulse was produced.

It was suspected that the cause of the poor Pockels cell performance might be that the electric field in it was not sufficiently uniform, due to the fact that the electrodes on the crystal's holder were about the same size as the crystal, which could lead to a nonuniform field due to edge effects. To solve this problem, a new Pockels cell holder was made which had larger electrodes. This did not improve performance, but it was found that decreasing the pressure on the crystal by loosening the new mount reduced the energy in the prelasing pulses by about one half, when the mount was as loose as was possible. The limiting factor in how loosely the crystal could be clamped was that the weight of the high-voltage cable connected to the mount put stress on the upper electrode which would cause the position of the crystal to shift if the mount was too loose. An effort was made to reduce this stress in the redesign of the electrode, but this was only partially successful.

In a final attempt to solve the prelasing problem, a cell filled with a saturable absorbing dye* was added to the cavity. Such dyes are often used on their own to produce passive Q-switching when accurate timing is not needed. They suffer from the drawback that the Q-switched pulses produced have a significant "jitter" in the time at which they are produced. It was hoped that by using a weak solution of the dye in addition to the Pockels cell Q-switch, enhanced cavity loss prior to Q-switching could be achieved without introducing extra jitter in the timing, because the Q-switch time would be controlled by the Pockels cell.

When dye of the appropriate concentration was placed in the cavity, some shots with no prelasing were observed. Unfortunately, after only a few shots the Q-switched light pulse began coming later and later, until eventually timing jitters as large as several microseconds were observed. Allowing the dye to "rest" for ten to fifteen minutes sometimes made it possible to fire one or two good shots before the jitter reappeared, but this limitation was unacceptable, and so the use of the saturable absorbing dye was abandoned.

As a final test, the extinction ratio of the Pockels cell was measured more accurately than had been done previously. The cell was placed between a plane mirror and a polarizer, and the intensity of helium-neon laser light reflected by this apparatus was measured. This approach reduces the possibility of error due to imperfect polarizer orientation. Interference between the HeNe beam and its reflections was also eliminated, to improve the stability of the output. The results are plotted in Figure 3.7.

* The dye used was Bis (4-dimethylaminodithiobenzil) nickel, dissolved in 1,2-dichloroethane. No attempt was made to determine the exact concentration used, because the concentration needed was expected to change with cavity alignment. The dye was prepared by diluting a saturated stock solution to about 1/25 of its original concentration, this ratio having been found by trial and error to be about ideal.

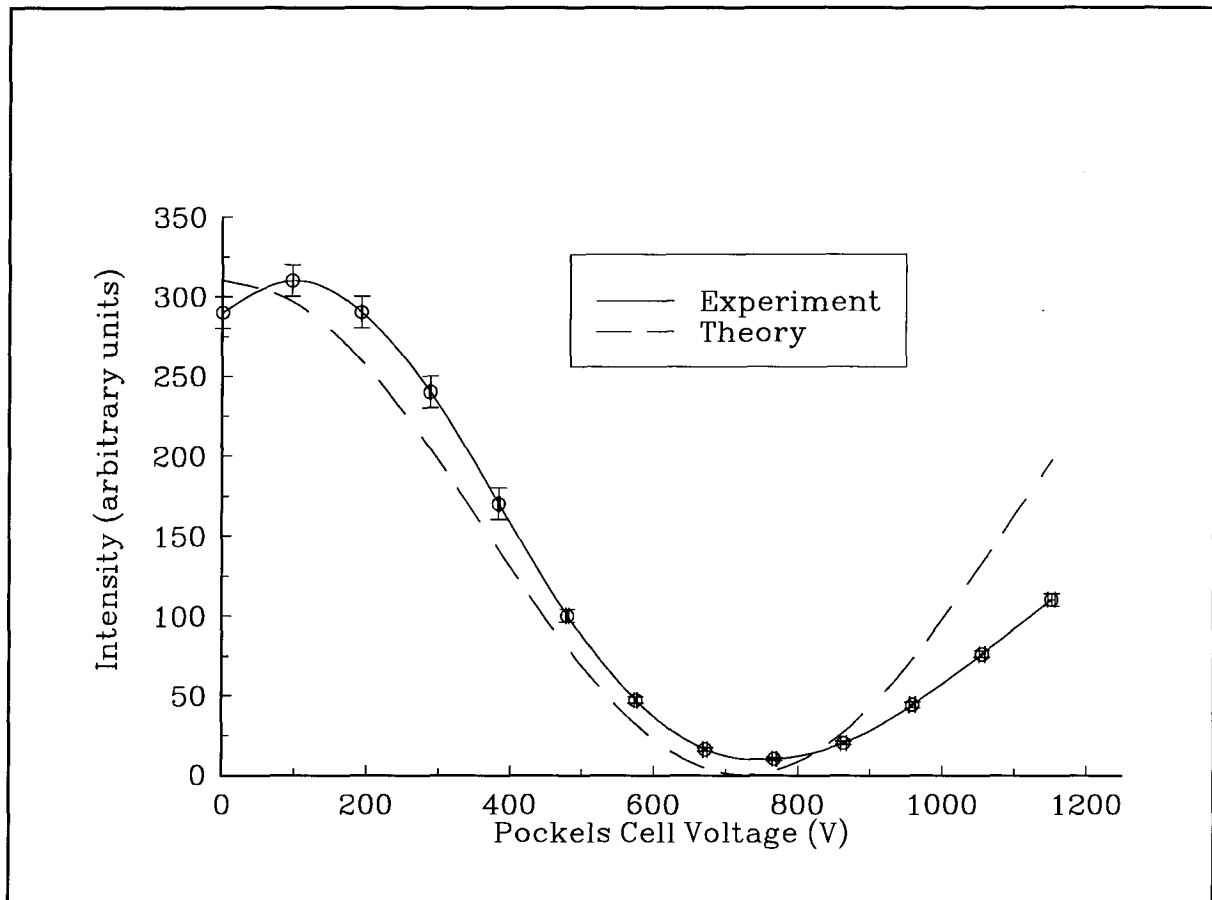


Figure 3.7: Observed and expected reflection of HeNe light by an apparatus consisting of a Pockels cell placed between a plane mirror and a polarizer. The theoretical curve is normalized to the same peak intensity as the observed data.

As shown, the output intensity was observed to peak at about 100 V, rather than at 0 V. This shift could be due to a static birefringence in the crystal, but introducing such an effect to the theoretical plot does not improve the overall fit to the data. The position of the minimum was within 40 V of the expected value in these measurements, but this position was observed to vary from time to time. Positions of the minimum as much as 150 V higher were observed. The extinction ratio of the data plotted is 31 ± 4 , which agrees reasonably well with the less accurate measurements reported on page 36.

The cause of the problem in the laser's performance has thus been identified, allowing the formulation of some possible solutions. These are discussed in the next chapter, which also contains a summary of the results reported in this thesis, and some other suggestions for improving the laser's performance.

Chapter 4

Conclusions

A Q-switched, cavity-dumped Nd:YAG laser system has been developed which is capable of producing 18 ± 2 mJ pulses with a full width at half-maximum of about 12 ns. While the pulse energy observed is more than half of the initial estimate of what the output energy should be, it is apparent that this estimate was too low, as there is over 100 mJ of energy being lost in prelasing which could in principle be recovered as useful output. The cause of this prelasing is that the Pockels cell used does not introduce enough loss to the cavity to counteract the high gain of the YAG rod.

Despite numerous attempts to improve the performance of the Pockels cell, it remained unsatisfactory. The loss introduced by the cell was measured as a function of applied voltage, and it was found that the extinction ratio was only 31 ± 4 . Problems with the shape of the loss curve which may be due to residual birefringence were also observed. It is possible that the cell's poor performance is caused by stress from its mounting altering the polarization of light in it via the elasto-optic effect, or that a more precise alignment than is possible with the current mount is needed. It is also possible that the crystal is simply defective.

In order to improve the performance of the laser, a new mount for the Pockels cell should be designed, in which the high-voltage connector is attached rigidly to the base of the mount rather than to the platform on which the crystal rests, as is done in the current design. Even if the resulting reduction in stress has no effect on the crystal's performance, this

change would greatly improve the ease and accuracy of alignment, especially if the mount allowed minute rotational adjustments of the crystal about more than one axis.

If this change does not bring the laser's performance up to a satisfactory level, the lithium niobate Pockels cell should be replaced by a KDP cell. These cells require a higher operating voltage and protection from atmospheric moisture, but they have been found in the past to be very effective electrooptic devices.

Another change which should be made at some point is that the spark gap used for triggering of the laser should be replaced. The new gap should have smaller main-gap electrodes, with as fine a thread as possible for adjusting the gap spacing. The design of this gap could also be much simpler than that currently in use, as there is no need to have the connections for separate circuits for Q-switching and cavity dumping, as in Figure 3.2. Alternatively, an avalanche transistor circuit could possibly be used for triggering in place of the spark gap. Such circuits have come into common use in laser triggering systems in recent years, and if transistors with a sufficiently fast switching time are available such a circuit could provide a very practical and robust alternative to spark gap triggering in this application. Compatibility with the spark gaps in the existing CO₂ laser system could be provided by attenuating the voltage of the trigger pulse they put out and using it to trigger the avalanche circuit directly. It should be possible to do this without introducing any excess jitter to the system, beyond that of the transistors themselves.

Finally, some solution to the problem of longitudinal mode control in an unstable resonator should be found, to improve the shot-to-shot energy stability of the laser. This might involve using a tilted plane etalon and then placing a lens at the output to adjust the collimation of the beam, or some other technique.

List of References

- [1] J. E. Geusic, H. M. Marcos, and L. G. Van Uitert, *Appl. Phys. Lett.* **4**, 182 (1964).
- [2] W. Koechner, *Solid-State Laser Engineering* (Springer-Verlag, New York, 1976).
- [3] A. Yariv, *Quantum Electronics, 3rd Edition* (Wiley, New York, 1989).
- [4] P. E. Dyer, in *The Physics and Technology of Laser Resonators*, ed. by D. R. Hall and P. E. Jackson (Hilger-IOP, Bristol, 1989).
- [5] A. E. Siegman, *Proc. IEEE* **53**, 277 (1965).
- [6] A. E. Siegman, *Lasers* (University Science Books, Mill Valley CA, 1986), Chap. 22.
- [7] F. J. McClung and R. W. Hellwarth, *J. Appl. Phys.* **33**, 828 (1962).
- [8] W. G. Wagner and B. A. Lengyel, *J. Appl. Phys.* **34**, 2040 (1963).
- [9] A. A. Vuylsteke, *J. Appl. Phys.* **34**, 1615 (1963).
- [10] R. C. Weidler, J. H. Burkhalter, and A. A. Vuylsteke, *J. Appl. Phys.* **38**, 4510 (1967).
- [11] H. Houtman and J. Meyer, *J. Appl. Phys.* **57**, 4892 (1985).
- [12] J. H. Goncz, *Instrument Soc. of America*, **5**, No. 1 [p. ?] (1966).
- [13] J. E. Murray and W. H. Lowdermilk, *J. Appl. Phys.* **51**, 3548 (1980).